Aqueous Solubility of Organic Salts. Investigating Trends in a Systematic Series of 51 Crystalline Salt Forms of Methylephedrine.

Lygia S. de Moraes, [†] Darren Edwards, [‡‡] Alastair J. Florence,[‡] Andrea Johnston,[‡] Blair F. Johnston,[‡] Catriona A. Morrison,[†] and Alan R. Kennedy[*†]

[†] WestCHEM, Department of Pure & Applied Chemistry, University of Strathclyde, Glasgow G1 1XL, Scotland.

[‡] CMAC, EPSRC Centre for Innovative Manufacturing in Continuous Manufacturing and Crystallisation, Technology and Innovation Centre, University of Strathclyde, Glasgow G4 0NR, Scotland.

[‡‡]Strathclyde Institute of Pharmacy and Biomedical Sciences, University of Strathclyde, Glasgow G4 0NR, Scotland.

Correspondence Address.

Dr Alan Kennedy, WestCHEM, Department of Pure & Applied Chemistry, University of Strathclyde, Glasgow G1 1XL, Scotland. Fax: (+44) 141-548-4822.

E-mail: a.r.kennedy@strath.ac.uk

Abstract

A dataset consisting of structures and aqueous solubility and melting point data for 51 salt forms of the phenylethylamine base methylephedrine is presented. Analysis showed correlation between solubility and melting point and between melting point of the salt and melting point of the parent acid, but no correlation of salt solubility with solubility of the parent acid. Identification of associations was aided by examining chemically sensible subgroups of the dataset, and this approach highlighted significantly different relationships between solubility and melting point for these subgroups. Thus, for example, the expected negative correlation between solubility and melting point was found for 24 anhydrous benzoate salts, but a positive correlation observed for 8 halide salts. Hydrated forms were anomalous. Packing analysis identified groups of structures that were isostructural with respect to cation packing. Correlation between solubility and melting point was found to be greatest within these isostructural groups, implying a role for packing structure in determining solubility.

Introduction

In industry salt forms of active pharmaceutical ingredients (APIs) are routinely screened with a view to finding a solid-state form that enhances some useful physicochemical property of the API. Often the main such property of interest is the aqueous solubility of the API, due to the relationship of solubility to dissolution rate and hence to bioavailability.[1] However, the links between salt form, solid-state structure and solubility (or indeed other properties) are currently poorly understood, making it largely impossible to accurately predict that a given salt form of an API will be more or less soluble than another. Many suggested structure-property links in the literature are valid only for the immediate system described and lack reliable transferability to a wider sphere. This lack of generality is illustrated by the apparently contradictory observations that simply adding polar groups to API species can lead to both an increase in aqueous solubility,[2] and to a decrease in aqueous solubility.[3] Anderson and Flora point out that chemical changes that favour hydration and aqueous solubility, such as increasing charge density or adding polar groups, also tend to increase intermolecular bonding in the solid-state and thus favour decreased solubility.[4] Exacerbating this problem is a general lack of large, systematically related structural datasets of salt forms of an API where reliable phase-specific physicochemical

data is also available. Such datasets should be beneficial to understanding structure/property relationships but many early studies on solubility of molecular salts contain no structural data.[1,5,6] More recently, reporting structural data alongside physical property data for series of salt forms has become more common, but such studies still typically report relatively small numbers of structures.[7-14] Some larger structural datasets are now available, such as the aqueous solubility data reported for 36 benzoate salts,[15] and the work of Davey and co-workers who structurally characterised 17 salt forms of the phenylethylamine base ephedrine and thoroughly analysed the inter-relationships of several properties including solubility.[16,17] Our interest in structure-solubility relationships and the existence of priorsystematic structural analysese of phenylethylamine bases,[15,18,19] including the work of Davey, prompted us to investigate solubility relationships in salt forms of methylephedrine. Herein we report aqueous solubility measurements on 51 salt forms, all of which have been characterised by single crystal diffraction and report on the relationships of solubility with, amongst other things, melting point, structure and properties of the parent acids.

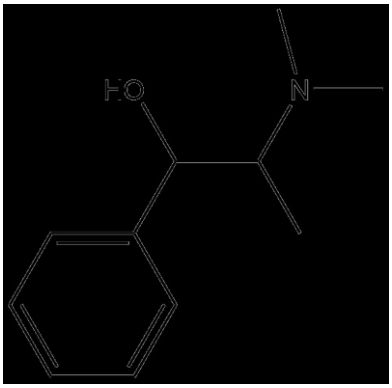

Scheme 1. Methylephedrine free base.

Experimental

Melting Points. Melting points were collected in triplicate using a Buchi B-545 automatic melting point apparatus. The average values obtained are presented in Table 1. This Table also gives the cation names used throughout.

Solubility measurements. Powder samples of the salts were first checked for purity by powder diffraction, see below. Approximately 0.5 g of each salt was used to produce saturated aqueous solutions (typically with 1 to 2 cm^3 of deionised water). These slurries were stirred in an

incubator at 25 ^{o}C for three days to ensure equilibrium had been reached. The saturated solution was then extracted from the slurry by centrifugal methods (6000 rpm for 10 mins).

The solubility was determined by measuring the UV absorbance of the cation. A calibration curve was established for methylephedrine dissolved in DMSO, within the linear domain of the Beer-Lambert law. Five points within the 0 to 1 absorbance domain were used to establish a linear relationship between the absorbance of the cation and the molarity, with a R^2 >99.9 %. (An independent calibration curve using salt forms rather than the free base was also constructed and comparison of the two methods showed that they gave identical results). The weighing and dilution of the calibration was checked by the preparation of quality control standards at 100 % and 10 % with an acceptability limit of 10 %. All salt solubility measurements were obtained in duplicate by diluting the saturated solution with DMSO until the absorbance fell within the linear response of the calibration curve. DMSO was used in preference to water to prevent potential problems with salting out.

Solubility analysis was performed using an Agilent 1200 UPLC, with a Waters X-Bridge column (C18, 5 μm, 2.1 x 50 nm). Measurements were made with a column temperature of 60 ^{o}C and a gradient mobile phase at a flow rate of 1.00 ml/min, commencing with phase A (0.1 % NH_4 + H_2O, milli Q) and phase B (0.1 % NH_4 + ACN, HPLC grade) at 95 % and 5 % respectively for 0 minutes. The gradient was then introduced over a period of 2 minutes to reach a final ratio of 5 % A and 95 % B, which was held for a further 0.3 minutes to insure all analytes had eluted form the column. The quantitative analysis of cation in the salt sample was determined using a UV-Vis detector at both 230 nm and 254 nm. The data was collected and processed using Chromeleon software.[20] Table 1 shows the average values achieved for the solubility measurements, given in mol dm^{-3} of the cation.

Table 1. Measured aqueous solubility and melting points with definition of abbreviations used throughout.

Cation →	Enantiopure MePD			Racemic RMePD		
Anion ↓	Solubility (mol dm^{-3} cation)	Standard Deviation	Melting Point (°C)	Solubility (mol dm^{-3} cation)	Standard Deviation	Melting Point (°C)
2AB 2-aminobenzoate	2.354	0.033	106.3			
2CB 2-chlorobenzoate				0.434	0.001	131.0
2FB 2-fluorobenzoate	1.235	0.008	132.6			
2HB 2-hydroxybenzoate	0.190	0.000	130.0			
2NB 2-nitrobenzoate	0.313*	0.019	80.1			
3AB 3-aminobenzoate	1.621	0.037	142.1			
3CB 3-chlorobenzoate	0.176*	0.000	75.5	0.138	0.003	135.1
3FB 3-fluorobenzoate	0.344	0.006	138.2	0.524	0.010	116.0
3HB 3-hydroxybenzoate				0.496	0.014	143.2
3NB 3-nitrobenzoate				0.047	0.001	157.0
4AB 4-aminobenzoate	1.499	0.135	130.5	1.687	0.098	131.0
4CB 4-chlorobenzoate	0.052	0.003	177.5	0.035**	0.001	163.5
4FB				0.201	0.003	133.9

Cation →	Enantiopure MePD			Racemic RMePD		
Anion ↓	Solubility (mol dm^{-3} cation)	Standard Deviation	Melting Point (°C)	Solubility (mol dm^{-3} cation)	Standard Deviation	Melting Point (°C)
4-fluorobenzoate						
4HB 4-hydroxybenzoate	0.440	0.006	160.3	0.885**	0.009	142.3
4HBS 4-hydroxybenzene Sulfonate	1.173	0.134	147.6	1.185*	0.035	120.7
4NB 4-nitrobenzoate	0.128	0.002	161.7	0.066	0.005	168.0
Adp H-adipate				1.704	0.018	110.3
BF4 tetrafluoroborate	2.461	0.005	112.2			
Br bromide	0.596	0.004	177.0	0.646	0.047	184.0
BS Benzene sulfonate				2.712	0.116	103.9
Bz benzoate	0.327*	0.006	83.2			
Cl chloride	2.443	0.024	194.0	1.349	0.022	211.8
EDS ethylenedisulfonate	3.552	0.072	102.2	0.527*	0.007	98.4
Free Base	0.048	0.001		0.102**	0.001	
I polyiodide	0.323	0.004	85.5	0.495	0.014	140.8
LTar l-H-tartrate	2.521	0.044	83.6			
Male malate	0.939	0.029	125.7	1.270	0.031	131.3

Cation →	Enantiopure MePD			Racemic RMePD		
Anion ↓	**Solubility (mol dm^{-3} cation)**	**Standard Deviation**	**Melting Point (°C)**	**Solubility (mol dm^{-3} cation)**	**Standard Deviation**	**Melting Point (°C)**
Malon **Malonate**	3.957	0.194	113.6	3.623	0.198	114.9
MD **mandelate**	1.821*	0.063	123.2			
mTol **3-toluate**				1.387	0.035	110.3
oTol **2-toluate**	1.663	0.102	100.7	0.286	0.002	132.7
pTol **4-toluate**	0.128	0.002	160.0	0.109**	0.002	142.9
RMD **Rac-mandelate**	3.415	0.083	102.9	4.132	0.072	120.5
RTar **Rac-H-tartrate**				3.774	0.308	128.3
Suc **H-succinate**	2.287	0.037	102.8	1.943		85.0

* Hydrated crystal forms. ** Racemic conglomerates.

Single Crystal Diffraction. Crystals were grown from aqueous solution. Measurements were made at low temperature using graphite monochromated radiation. Structures were solved by direct methods and refined to convergence against F^2 using all independent reflections.[21,22] Selected crystallographic and refinement parameters are given in Table 2. Full data has been deposited in CIF format as CCDC 1533576 through to CCDC 1533596. This data can be obtained free of charge from the Cambridge Crystallographic Data Centre via www.ccdc.cam.ac.uk/data_request/cif.

Table 2a. Selected Crystallographic Data for Salts Containing (-) Methylephedrinium (**MePD**).

Salt form	**Chemical formula, MW**	**Space group**	**Cell lengths *a, b, c* (Å)**	**β (°), V (Å^3), Z**	**R_1, wR_2, S**
2AB	$C_{11}H_{18}NO$, $C_7H_6NO_2$ 316.39	$P2_1$	6.9241(2) 13.8555(4) 8.7686(3)	97.216(3) 834.57(4) 2	0.0302 0.0690 1.016
2FB	$C_{11}H_{18}NO$, $C_7H_4FO_2$ 319.37	$P2_1$	5.7285(2) 14.8236(16) 9.7213(3)	97.952(4) 817.57(10) 2	0.0331 0.0663 0.934
2HB	$C_{11}H_{18}NO$, $C_7H_5O_3$ 317.37	$P2_12_12_1$	9.4432(2) 11.6437(4) 15.0684(5)	90 1656.83(10) 4	0.0377 0.0600 0.814
3AB	$C_{11}H_{18}NO$, $C_7H_6NO_2$ 316.39	$P2_1$	5.8225(2) 13.4434(4) 21.0918(7)	95.723(3) 1642.71(9) 4	0.0593 0.1449 1.023
4AB	$C_{11}H_{18}NO$, $C_7H_6NO_2$ 316.39	$P2_12_12_1$	9.2790(2) 13.3031(3) 13.8797(3)	90 1713.30(7) 4	0.0279 0.0684 1.072
BF4	$C_{11}H_{18}NO$, BF_4 267.07	$P2_12_12_1$	7.8841(2) 11.4446(3) 14.5177(5)	90 1309.94(7) 4	0.0311 0.0643 0.935
LTar	$C_{11}H_{18}NO$, $C_4H_5O_6.H_2O$ 347.36	$P2_1$	10.6983(17) 7.4656(11) 11.6355(17)	112.494(17) 858.6(2) 2	0.0394 0.0716 0.954
MD	$C_{11}H_{18}NO$, $C_8H_7O_3.H_2O$ 349.42	$P2_1$	9.9766(3) 5.7644(2) 15.9095(6)	93.403(3) 913.33(5) 2	0.0378 0.0754 1.028
RMD	$C_{11}H_{18}NO$, $C_8H_7O_3$	$P2_12_12_1$	7.4095(4) 9.8209(6)	90 1745.28(18)	0.0340 0.0783

	331.40		23.9842(15)	4	0.960
Suc	$C_{11}H_{18}NO$, $C_4H_5O_4$ 297.34	$P2_12_12_1$	6.0939(3) 14.0600(8) 17.8802(13)	90 1531.98(16) 4	0.0573 0.1348 0.994

Table 2b. Selected Crystallographic Data for Salts Containing (+/-) Methylephedrinium (**RMePD**).

Salt form	**Chemical formula, MW**	**Space group**	**Cell lengths *a*, *b*, *c* (Å)**	**Cell β (°), V (Å^3), Z**	**R_1, wR_2, S**
3HB	$C_{11}H_{18}NO$, $C_7H_5O_3$ 317.37	$P2_1/c$	10.2539(9) 14.9782(16) 11.2503(10)	92.194(7) 1726.6(3) 4	0.0369 0.0702 0.739
3NB	$C_{11}H_{18}NO$, $C_7H_4O_4$ 346.38	C2/c	25.3221(5) 5.7669(1) 23.6945(6)	96.453(2) 3438.19(13) 8	0.0335 0.0903 1.067
4AB	$C_{11}H_{18}NO$, $C_7H_6NO_2$ 316.39	Pbca	9.0458(2) 14.9474(3) 24.8220(6)	90 3356.21(13) 8	0.0381 0.0887 1.071
4FB	$C_{11}H_{18}NO$, $C_7H_4FO_2$ 319.37	$P2_1/c$	12.5372(4) 13.4436(4) 10.3673(2)	105.903(2) 1680.48(8) 4	0.0475 0.1272 1.064
ADP	$C_{11}H_{18}NO$, $C_6H_9O_4$ 325.40	$P2_1/c$	5.8543(3) 23.7826(10) 12.6197(6)	103.349(5) 1709.57(14) 4	0.0341 0.0722 0.834
EDS	$C_{11}H_{18}NO$, $[C_2H_4O_6S_2]_{0.5}$ .H_2O 292.37	P-1	5.7707(2) 10.6056(6) 13.0464(5)	[a] 719.52(6) 2	0.0305 0.0792 1.073

I	$C_{11}H_{18}NO$, [I].0.5I_2 434.06	C2/c	12.7306(2) 8.9883(2) 24.9567(5)	96.364(2) 2838.11(10) 8	0.0154 0.0312 1.145
mTOL	$C_{11}H_{18}NO$, $C_8H_7O_2$ 315.40	C2/c	24.371(5) 6.0222(9) 23.684(3)	95.240(17) 3461.5(10) 8	0.0525 0.1448 0.919
RMD	$C_{11}H_{18}NO$, $C_8H_7O_3$ 331.40	$P2_1/c$	13.0646(7) 9.5474(4) 13.9012(5)	91.572(5) 1733.29(13) 4	0.0955 0.3611 1.286
Suc	$C_{11}H_{18}NO$, $[C_4H_4O_4]_{0.5}$ 238.31	$P2_1/c$	16.0654(7) 8.1278(3) 9.7638(3)	92.226(3) 1273.96(8) 4	0.0549 0.1127 1.047
RTar	$C_{11}H_{18}NO$, $C_4H_5O_6$ 329.35	$Pbc2_1$	7.9133(5) 10.1443(5) 40.028(4)	90 3213.2(4) 4	0.0875 0.2514 1.053

[a] α, β, γ = 106.273(4), 99.721(3), 103.950(4) °.

Powder Diffraction. Measurements were made with a Bruker D5000 diffractometer using Cu Kα radiation (λ = 1.5418 Å) and operating in flat-plate mode. The data was collected at room temperature with a 2θ range of 4.0 º to 35.1 º. Unit cell parameters identified by SXD methods were refined against collected data using the Pawley method as implemented in DASH.[23] Data are presented in the ESI. X-ray powder diffraction was used to check that the measured single crystal diffraction structures were representative of the bulk material. The samples were first ground to achieve a fine powder which was analysed to check the purity of the bulk sample. After the saturated solution had reached equilibrium (see solubility measurements, below) the wet powder recovered was analysed to check the phase of the material for which solubility was recorded. Samples were presented "wet" in an attempt to prevent unwanted phase transitions. A phase change was observed to occur during the slurry experiment for the **EDS** salt of **RMePD**.

Results and Discussion; Aqueous solubility was determined by initially forming slurries of salt forms of enantiopure (-) methylephedrine (**MePD**) or racemic methylephedrine (**RMePD**), such that the saturated solution phases were in equilibrium with the solid-salt phases. Solubility measurements were only included in this work where PXRD indicated that the solid phase present in the slurry matched that of a known SXD determined structure for a methylephedrine containing compound. This gave a total of 53 aqueous solubility values, each matched to a specific crystal phase. These were for 26 enantiopure **MePD** salts, 22 racemic **RMePD** salts, 3 for salt forms of **RMePD** that were racemic-conglomerates, and both the enantiopure and racemic-conglomerate forms of the free base, see Table 1. (Note, a racemic-conglomerate consists of a mechanical mixture of equal amounts of (-) and (+) crystals of methylephidrine).[24] Six of the salt forms were found to be hydrated species. Of the 48 independent salt single crystal structures, we originally described 28 in reference 18 and 20 are reported here for the first time.

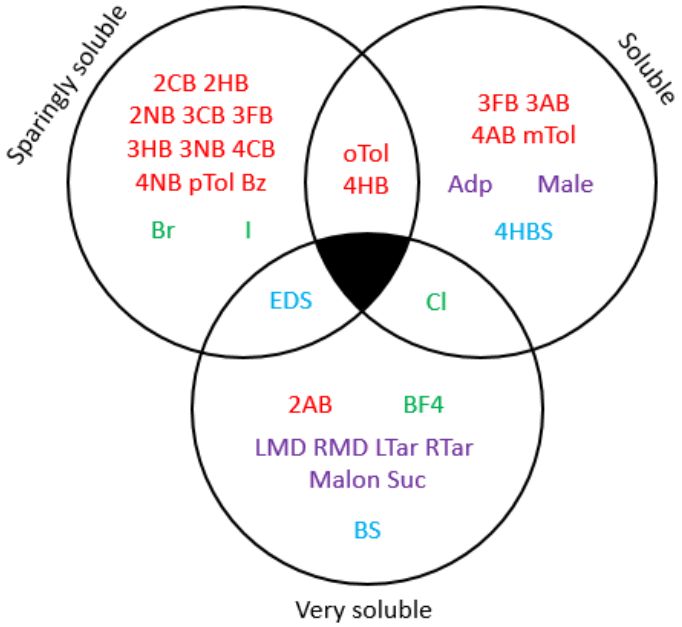

Figure 1. Solubility classifications of salt forms of methylephedrine. Red = benzoate-derived anions, light blue = sulfonate anions, purple = other carboxylate and dicarboxylate anions, green = inorganic anions. Entries in the regions where circles overlap correspond to those anions which give different solubility classes for the **MePD** and **RMePD** cations.

General trends in solubility for methylephedrinium salts with respect to cation type.

The enantiopure and racemic free base forms were found to have solubilities of 0.048 and 0.102 mol dm^{-3} of cation respectively. From Table 1, most of the salt forms were more soluble than these (range 0.035 to 4.132 mol dm^{-3}, a range covering 2 orders of magnitude) but **4CBMePd**, **4CBRMePd**, **3NBRMePD** and **4NBRMePD** were all less soluble than the racemic free base (0.035 to 0.066 mol dm^{-3}). Forms with *para*-toluate were also barely more soluble than free base. These lowest solubility forms are all salts of *para*- or *meta*-substituted benzoates. Figure 1 categorises solubility by anion. Solubility values were arbitrarily described as "sparingly soluble" (<0.75 mol dm^{-3}), "soluble" (0.75-1.75 mol dm^{-3}) or "very soluble" (>1.75 mol dm^{-3}). Most benzoate-derivative salts fit into the sparingly soluble category. It is interesting that all four of the aminobenzoate salts have much higher solubility than the typical benzoate, ranging from 1.499 (**4ABMePD**) to 2.354 mol dm^{-3} (**2ABMePD**). The aminobenzoates are the only benzoate anions herein that have a second easily ionisable group. Their parent acids are also known to be considerably more hydrophilic, as shown by lower logP values, than the other benzoates used. This line of reasoning does not stand further examination as the other benzoates used feature both relatively hydrophobic species that give high solubility (e.g. **oTol**) and relatively hydrophilic species that give low solubility (e.g. **2NB**).

The carboxylate salts (excluding benzoates) shown in Figure 1 tend to have higher solubilities within a wide range from 0.939 mol dm^{-3} for **MaleMePD** to 4.132 mol dm^{-3} for **RMDRMePD**. Although this category of anion features several dicarboxylates that may be expected to be highly soluble on the simple grounds of "number of polar groups", it is in fact the monocarboxylate (and hydrophobic arene bearing) rac-mandelate that gives the most soluble salt form of all. Of the remaining anion types, all bromide and polyiodide salts have relatively low solubility. The chloride salts have a much higher solubility, especially the enantiopure salt with a measured solubility of 2.443 mol dm^{-3}. This difference is interesting as the chloride and bromide crystals are isomorphous and isostructural. This observation is expanded on later. The last group of anions used, the sulfonates, has a wide range of solubility values despite being relatively few in number. The **EDS** anion has the widest range of values for a racemic/enantiopure

methylephedrine pair (compare 0.527 and 3.552 mol dm^{-3}). It is tempting to attribute this large difference to the fact that the low solubility racemic salt is a hydrate. It is well known that hydrated species have lower aqueous solubilities than anhydrous equivalents.[25] However, this hydrate/anhydrate comparison is strictly only valid when comparing otherwise identical species – and here we are comparing **MePd** and **RMePD**. That this is not a valid comparison is shown by comparing the other two pairs of compounds here that feature a hydrate and an anhydrous from, the salts of **3CB** and **4HBS**. Neither shows the same behaviour as **EDS** and indeed for **3CB** the hydrated enantiopure material is clearly more soluble than the anhydrous racemic species, Table 1. Davey has presented and analysed solubility data on a series of 17 salt forms of ephedrine.[17] In that work the **BS** salt of ephedrine was noted as being of markedly low solubility and it was reasoned that this was due to the hydrophobic phenyl group. This observation for ephedrine does not translate to methylephedrine, as **BSRMePD** is found in our very soluble category.

Comparison of enantiopure and racemic salt solubility measurements for methylephedrinium salts

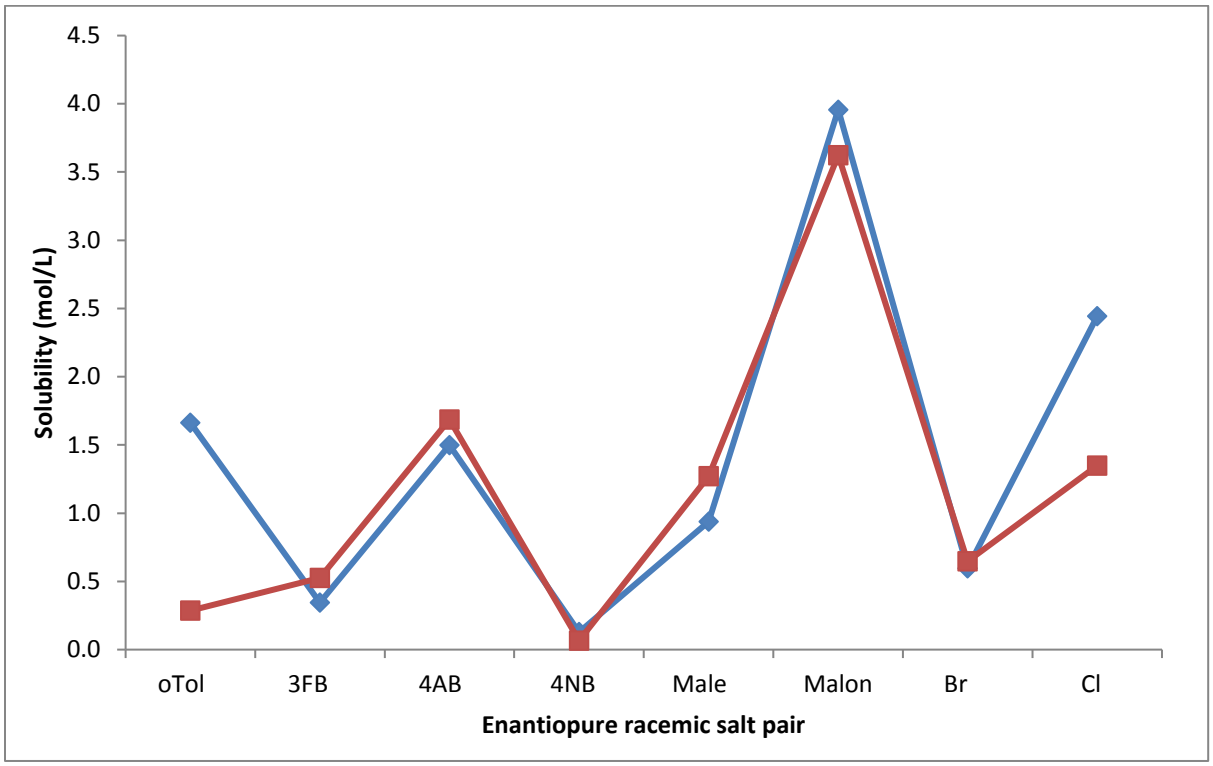

Figure 2. Comparing solubility of the 8 chemically identical enantiopure and racemic salt pairs. Red squares = racemic species, blue diamonds = enantiopure species.

Table 3. Solubility comparison data for pairs of chemically identical enantiopure and racemic forms.

Compound	**Enantiopure Solubility (mol dm^{-3} of MePD)**	**Racemic Solubility (mol dm^{-3} of RMePD)**	**Nature of Solid Racemate**
Free base	0.048	0.102	conglomerate
4HB salt	0.440	0.885	conglomerate
4CB salt	0.052	0.035	conglomerate
pTol salt	0.128	0.109	conglomerate
oTol salt	1.663	0.286	racemic crystal
3FB salt	0.344	0.524	racemic crystal
4AB salt	1.499	1.687	racemic crystal
4NB salt	0.128	0.066	racemic crystal
Male salt	0.939	1.270	racemic crystal
Malon salt	3.957	3.623	racemic crystal
Br salt	0.596	0.646	racemic crystal
Cl salt	2.443	1.349	racemic crystal

There are eight pairs of enantiopure **MePD** and racemic **RMePD** salts that are otherwise chemically identical and which can thus be directly compared with respect to their solubility, see Figure 2 and Table 3. These are composed of four benzoate-derived salts, two carboxylate salts and two halide salts. For these species, the average enantiopure solubility is 1.466 mol dm^{-3}, 22 % greater than the average racemic solubility of 1.181 mol dm^{-3}. Close examination of the data shows that the average difference is largely because of the large differences found for the **oTol** and **Cl** salts. The melting points of these two pairs are also very different with the more soluble species having lower melting points. However, the case of **3FB** shows that a large melting point difference does not need to mean a large difference in solubility, Table 1 and Figure 2. The

structural pairs for the **oTol** and **Cl** salts also have different cation conformations within each pair, see reference 18 for information on cation conformations, but so the **Male** pair and that does not show a large solubility difference. As enantiopure species cannot use all possible symmetry operations, they cannot access all the possible packing options open to racemic species. Thus it has been argued that enantiopure species must be packed less efficiently and less densely than racemic equivalents and that this must effect other properties such as enthalpy. This is Wallach's rule.[26] Experimentally, it has been shown that enantiopure species are indeed on average less dense than racemic equivalents,[18,27] but that this is caused by a small number of pairs that have large differences that favour more dense racemates. For any given individual pair, Wallach's rule does not necessarily hold as can be seen from the density values in the ESI and elsewhere. [18,27] This is reminiscent of the solubility results presented here.

The racemic free base and three of the racemic salts (**4HB**, **4CB** and **pTol**) do not from racemic crystals, instead racemic conglomerates of (-) and (+) forms are found. Note that the **4CB** and **pTol** species are isomorphic and isostructural. Meyherhoffer's double solubility rule states that the solubility of a racemic conglomerate should be double that of its enantiopure equivalent.[28] The free base obeys this rule, Table 3, as does the **4HB** salt. However, the two isostructural salts do not. This is presumably because the rule is intended for non-electrolytes (as the sharing of achiral anions in solution gives non-ideal behaviour).[29] All conglomerates reported here do have the expected lower melting points when compared to their enantiopure equivalents.[30]

Correlation of physical properties for (1R,2S)(-) methylephedrinium benzoate-derived salts.

In an initial attempt to find correlations between measured physical properties, solubilty, melting point, density and molecular weight of the salt forms and the solubility and melting point of the parent free acids were compared. Initially this was done using all 51 salt forms, but this gave unclear and unsatisfactory results, see as an example Figure 3. Instead data plots were constructed for chemically related groups. This was found to give clearer trends. The most interesting results are presented in this section with further analysis available in the ESI.

There were 14 enantiopure **MePD** benzoate-derived salts where solubility measurements were obtained and where the solid-state phase of the slurry was confirmed by PXRD. Of these 14 salts, three are monohydrates and the remainder are anhydrous. Prior work based on fundamental

considerations of dissolution as an equilibrium between solid and solution phases has shown that hydrated and anhydrous forms of materials should have different behaviour and thus these should be considered separately.[25,31]

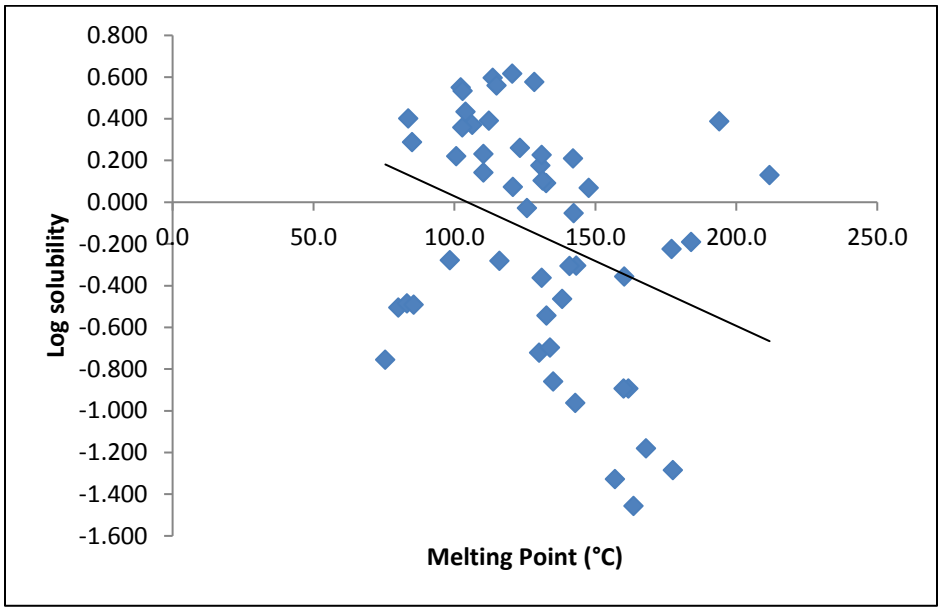

Figure 3. Illustration of an attempt to find correlations using all data in the sample, $R^2 = 0.1141$.

It is well known that melting point often correlates with log solubility and so this was the first relationship to be investigated.[17,32,33] For the enantiopure **MePD** benzoate derived salts, a plot of log solubility versus melting point showed a linear association between the values for the anhydrous salts, see Figure 4. As expected, the salts with the lowest melting points have the highest solubility. The values for the hydrated salts do not correlate to those of the anhydrous salts. Variable line fit and residual plots for this data are given in the ESI and show that the anhydrous data is homoscedastic (there is constant variance throughout all the data points) which is in agreement with the data being linearly correlated. This correlation, although containing a large associated error, is similar to other reported correlations which contain fewer data points.[32,33]

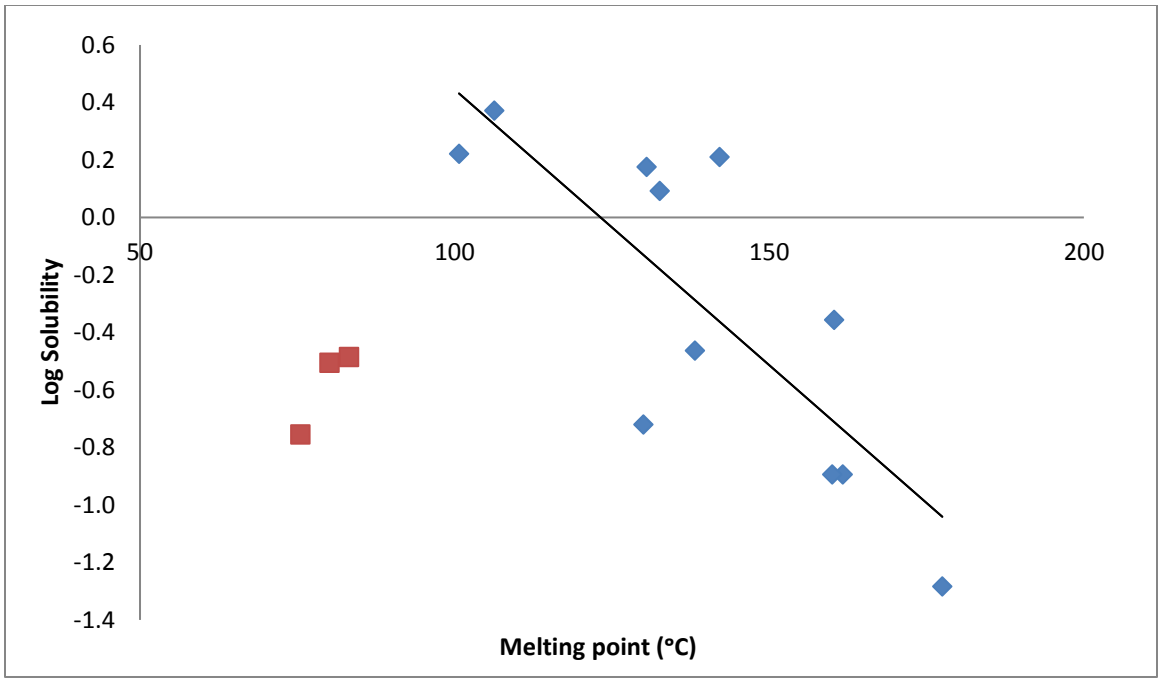

Figure 4. Plot of log solubility versus melting point of salt for **MePD** benzoate-derived salts. Here and elsewhere, the equation given for the best fit line does not include the points for the hydrate structures (red squares) . Equation for line, log y = -0.0192x + 2.3617. R^2 = 0.6381. Error on gradient 0.0048, error on intercept 0.6824.

For the **MePD** benzoate species a correlation was also found between the melting point of the parent free acids and the melting points of the salts formed from these, with high melting point free acids giving generally higher melting point salts, see Figure 5. Similar associations have been discussed by Gould.[32] Analysis given in the ESI confirms the data is homoscedastic. As might be expected, the hydrated species do not lie on this trend line.

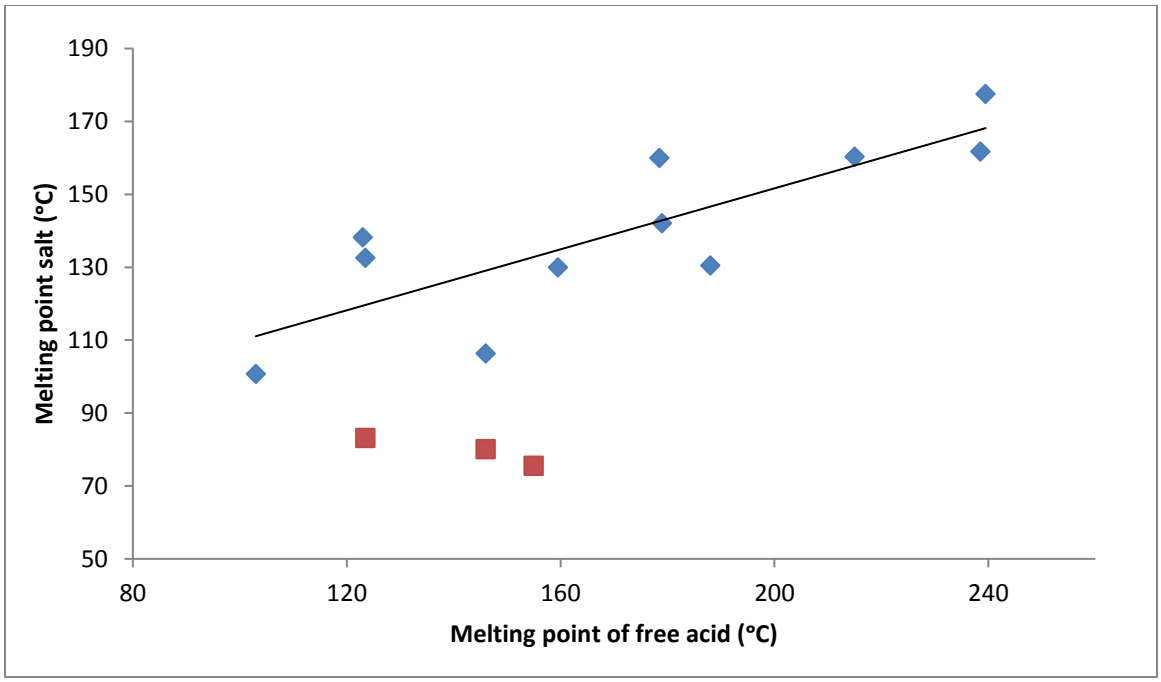

Figure 5. Plot of melting point of salt versus melting point of free acid for **MePD** benzoate-derived salts. Hydrate structures are red squares . Equation for line, y = 0.4182x + 68.005. R^2 = 0.6694. Error on gradient 0.0980, error on intercept 17.409.

As associations were found between melting point of salt and solubility and between melting point of free acid and melting point of the salt, we also examined possible correlation between melting point of the free acid and the solubility of the salt. Figure 6 shows a rough trend with high melting free acids giving low solubility salts, but this cannot be said to be a linear relationship.

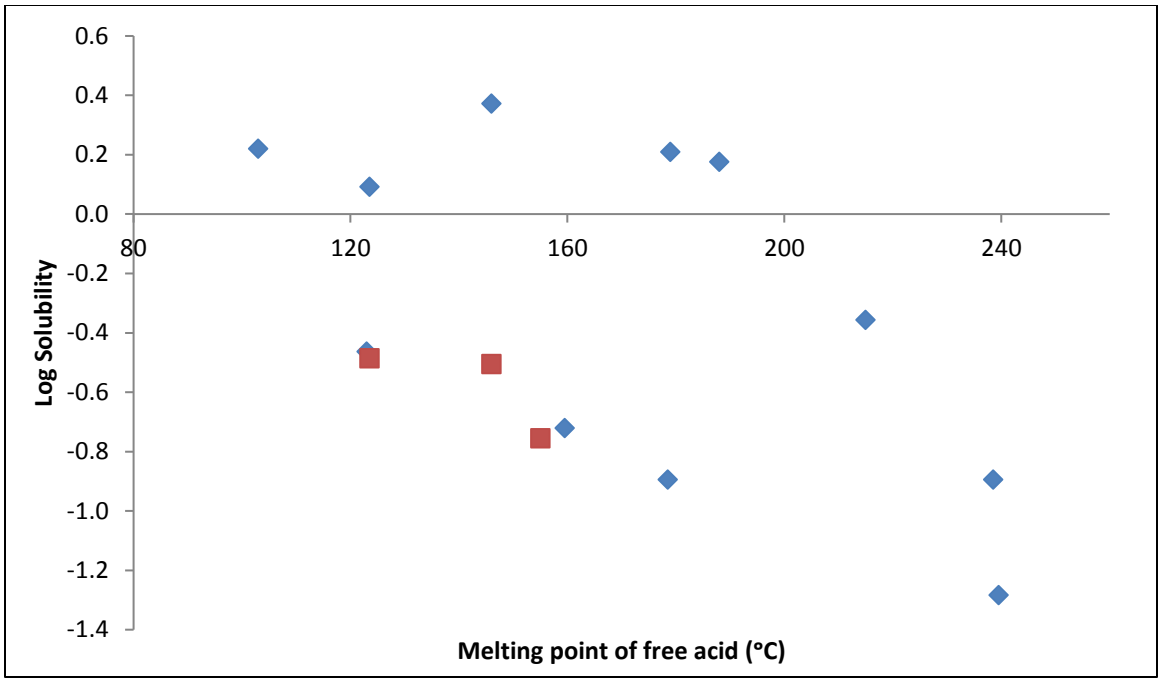

Figure 6. Plot of log solubility of salt versus melting point of free acid for **MePD** benzoate-derived salts. Blue diamonds represent anhydrous salt forms and red squares represent hydrated salt forms.

In other analyses for the 14 benzoate-derived salts of **MePD,** only a weak association was observed between solubility and molecular weight and no associations were found between density and either melting point or log solubility, see ESI. Nor was any association found between solubility of the salt and solubility of the parent free acid, Figure 7. This last observation is surprising because many previous studies have shown correlation between these two features for both salt and cocrystal forms.[15,34, 35] Measurement of solubility is notoriously variable and observed results are highly dependent upon method used.[36] The free acid solubility values used here were averages taken from a literature compendium rather than measured using a similar method to that used for the salt forms.[36] However, it is hard to see how even gross errors due to mismatch between techniques could compensate for the complete lack of association shown in Figure 7.

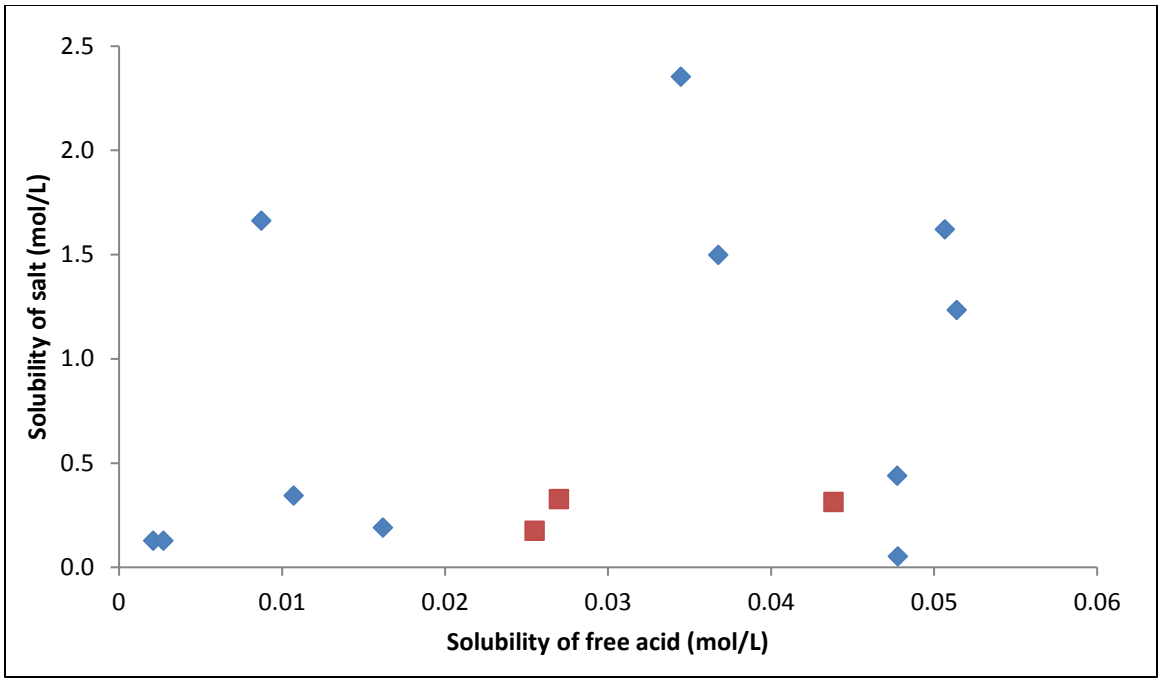

Figure 7. Plot of solubility of salt versus solubility of free acid for **MePD** benzoate-derived salts. Blue diamonds represent anhydrous salt forms and red squares represent hydrated salt forms.

Correlation of physical properties for (+/-)methylephedrinium benzoate derived salts.

The same analyses as above were also performed for the racemic **RMePD** salts of benzoate-derivatives. There are 13 salts that are to be considered in this group. These consisted of 10 racemic crystalline anhydrous salts and three salts that spontaneously resolved to form racemic conglomerates. Similar associations and lack of associations were found as for the enatiopure **MePD** salt forms, see Figures 8 to 11 and ESI.

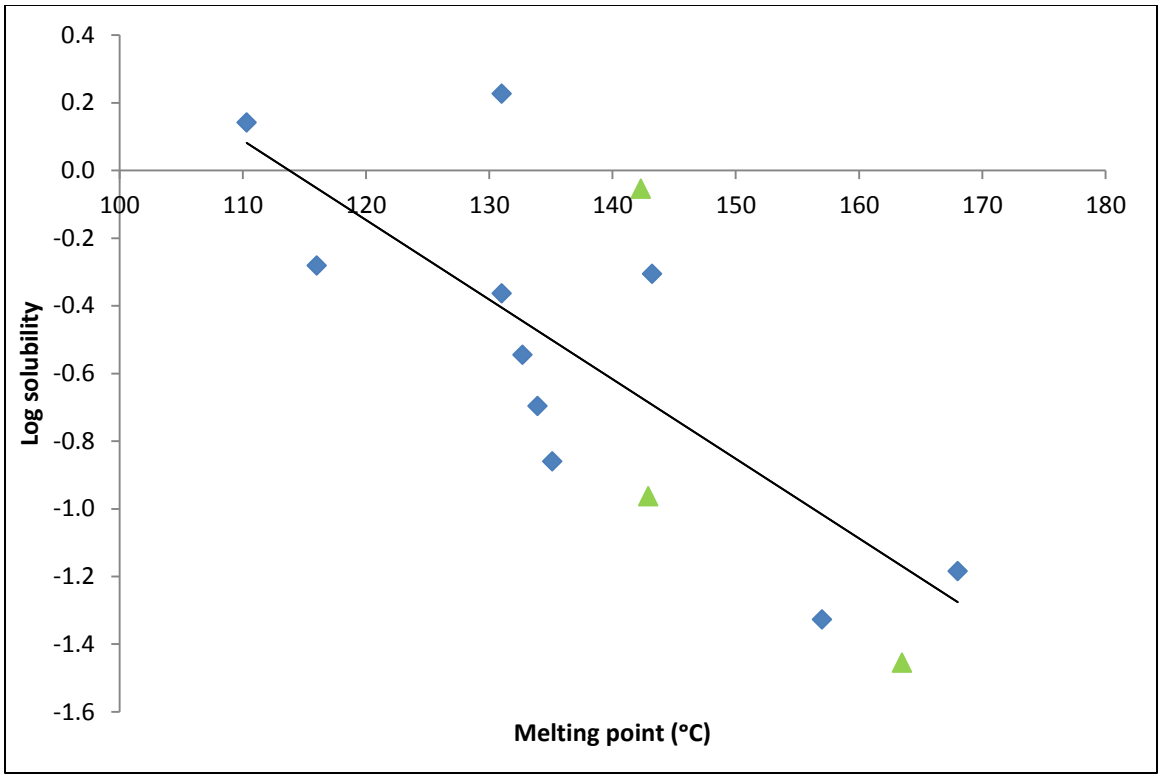

Figure 8. Plot of log solubility versus melting point of salt for **RMePD** benzoate-derived salts. Blue diamonds represent anhydrous salt forms and green triangles represent conglomerate species. Equation for line, log y = -0.0253x + 2.9294. $R^2 = 0.6195$.

As seen for the enantiopure forms above, the melting point of salt and log solubility data shows association, Figure 8. The racemic crystal and racemic-conglomerate data all appear to fit the same line. It was found that the graphs produced for the anhydrous enantiopure and racemic methylephedrinium salts are equivalent within the errors of the data and therefore all the data can be collated together. This has been shown in Figure 9.

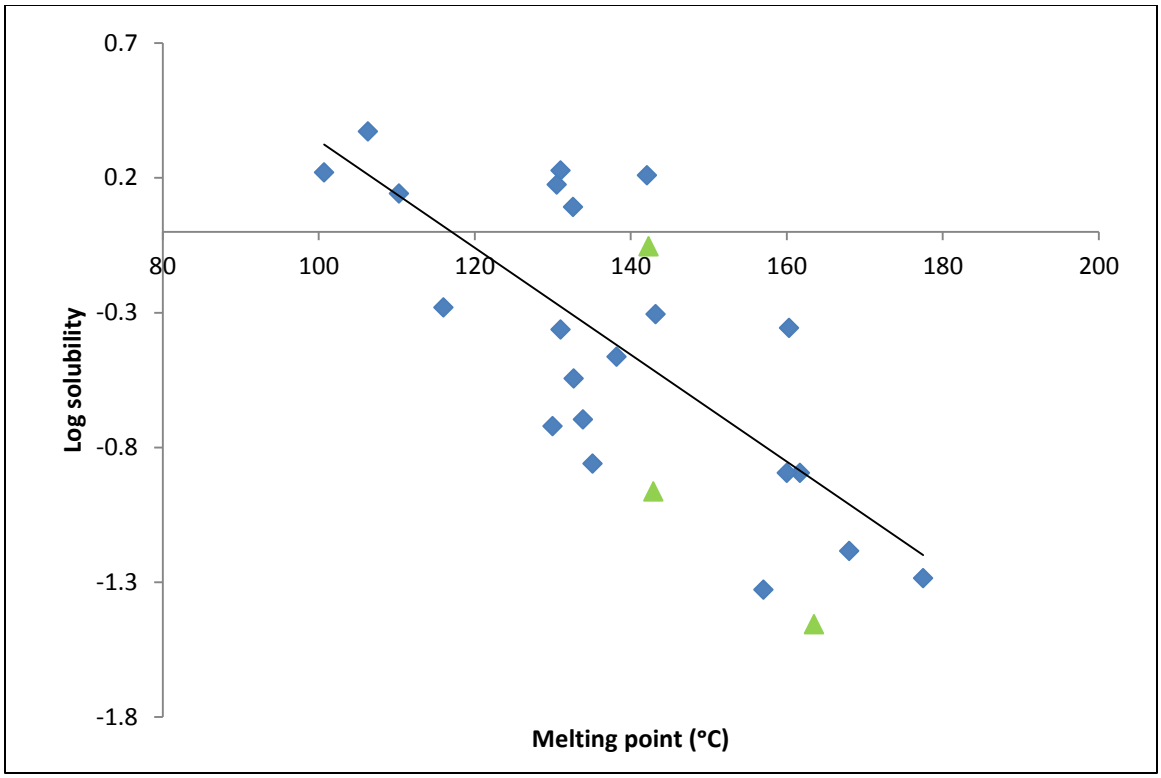

Figure 9. Combined plot of log solubility versus melting point of salt for **MePD** and **RMePD** benzoate derived salts. Blue diamonds represent anhydrous salt forms and green triangles represent conglomerate species. Equation for line, log y = -0.0198x + 2.3203. R^2 = 0.5660. The errors on the gradient and intercept are now 0.0038 and 0.5331 respectively.

The other data that shows a reasonable linear correlation for the **RMePd** salts is a comparison of the melting points of the free acids and the melting points of the salts. Here again the data for the **MePD** and **RMePD** compounds matches and so a combined graph can be produced, Figure 10. Again, the hydrated data is excluded and the conglomerate data is included.

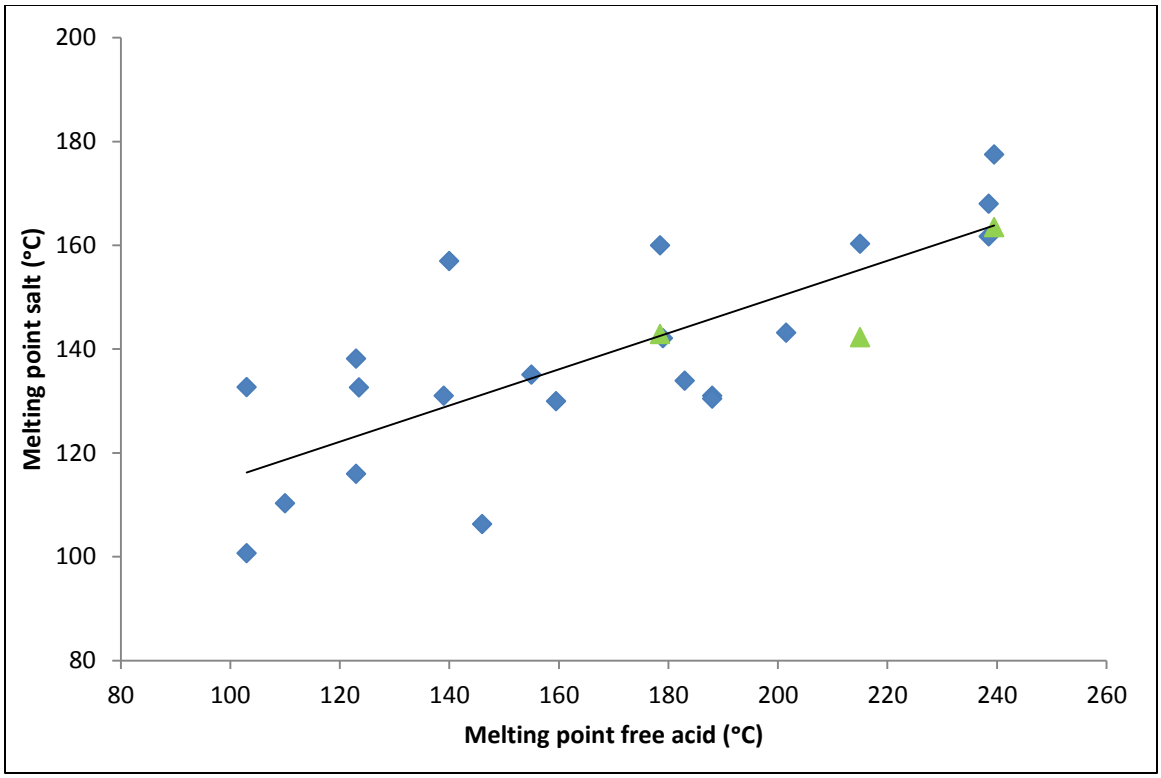

Figure 10. Combined plot of melting point of salt versus melting point of free acid for **MePD** and **RMePD** benzoate-derived salts. Blue diamonds represent anhydrous salt forms and green triangles represent conglomerate species. Equation for line, $y = 0.3483x + 80.372$. $R^2 = 0.5764$.

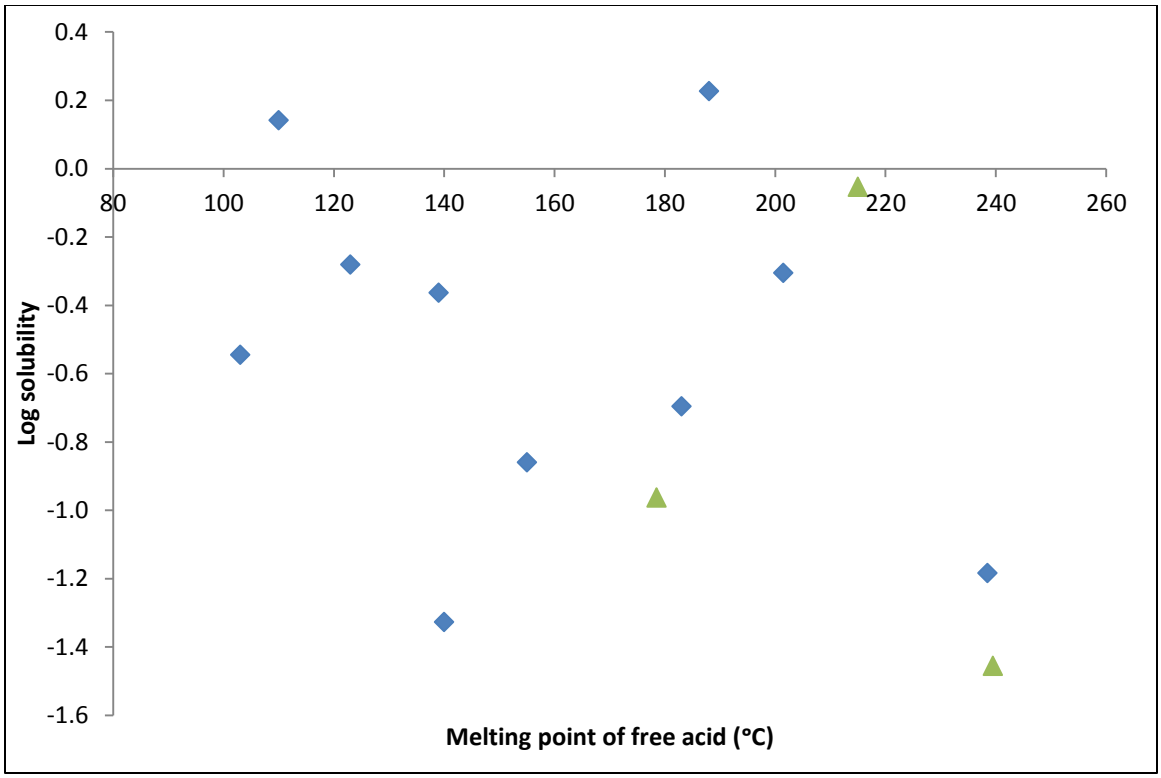

Figure 11. Plot of log solubility versus melting point of free acid for **RMePD** benzoate-derived salts. Blue diamonds represent anhydrous salt forms and green triangles represent conglomerate species.

Correlation of melting point and solubility for methylephedrinium sulfonate, carboxylate and halide salts.

The benzoate-derived anions discussed above formed a relatively large and systematically variable subset of data. The remaining samples (sulfonate, carboxylate and halide salts) formed smaller and/or much more chemically diverse groupings. We believe that these features hindered identification of associations. As it has been shown that the enantiopure and racemic methylephedrine salts of benzoate anions can be analysed together, all further analysis combined **MePd** and **RMePd** results in order to increase the number of data points in the analyses. Figures 12 and 13 show the results for examining melting point and salt solubility for the carboxylate and sulfonate groups respectively. These groups illustrate the difficulty experienced even where a reasonably strong correlation is expected. Both roughly hold to the concept of low solubility

being associated with high melting point, but the 12 carboxylate points cover such a range of chemical types (monocarboxylates, dicarboxylates, anhydrous and hydrated, 1:1 salts and 2:1 salts) that a lack of uniformity is unsurprising. Meanwhile there are only 5 sulfonate examples, of which two are hydrated. Again, this makes coming to an unambiguous conclusion difficult. It may be that measuring more data for materials that form systematic carboxylate or sulfonate series similar to the benzoate series would aid identification of strong correlations.

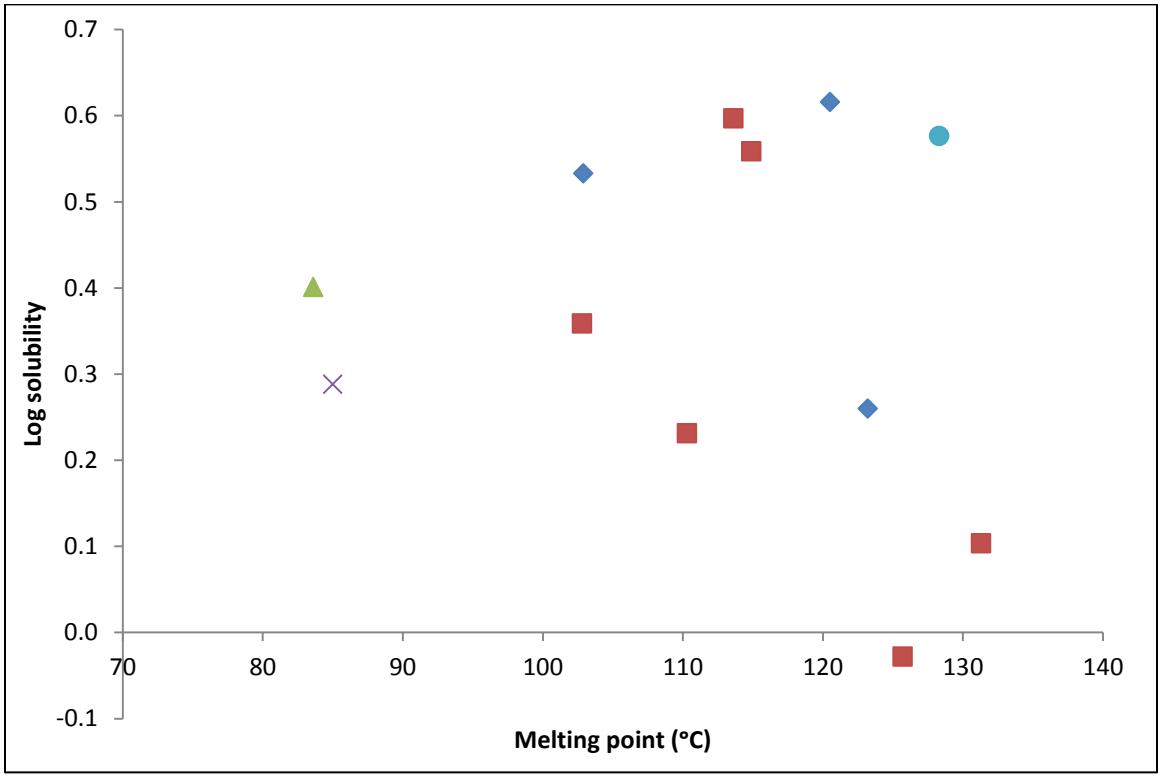

Figure 12. Plot of log solubility versus melting point of salt for carboxylate salts. Blue rectangle represent monocarboxylate salts, red square represent dicarboxylate anhydrous salts, green triangle represents dicarboxylate hydrated salt, purple cross represents two to one salt and blue circle represents co-crystal.

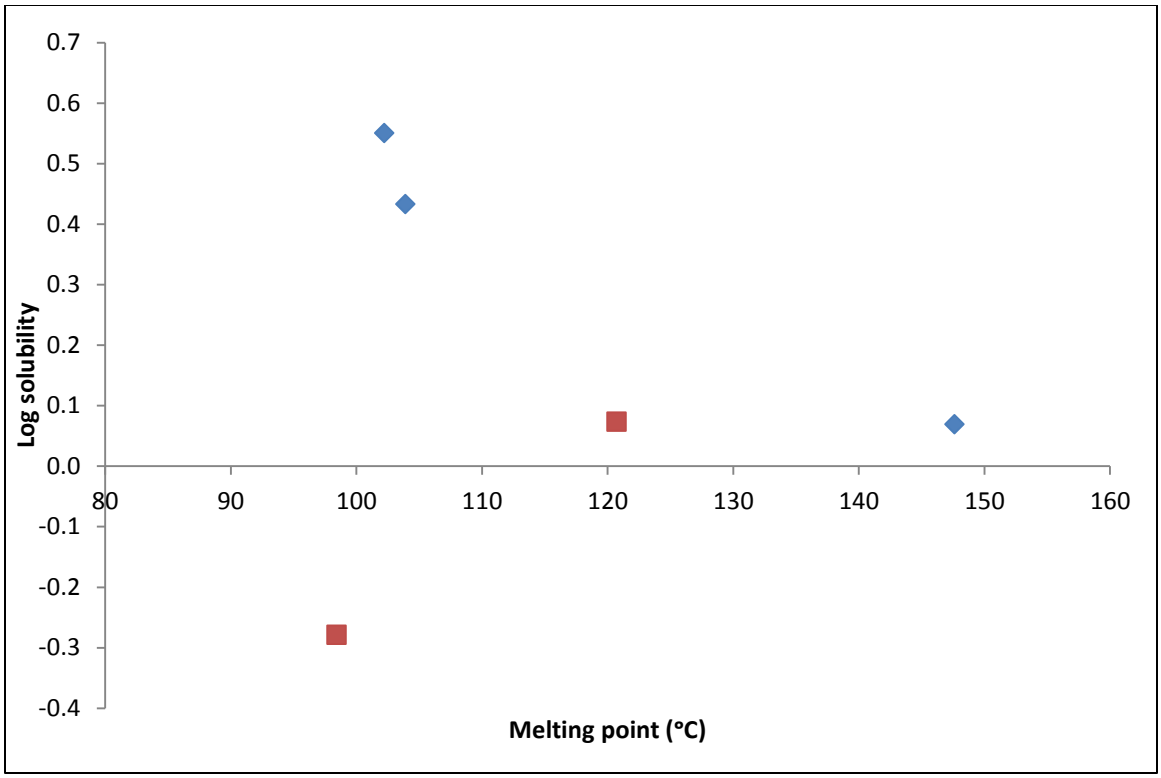

Figure 13. Plot of log solubility versus melting point of salt for sulfonate-derived salts. Blue rectangles represent sulfonate anhydrous salts and red squares represent sulfonate hydrated salts

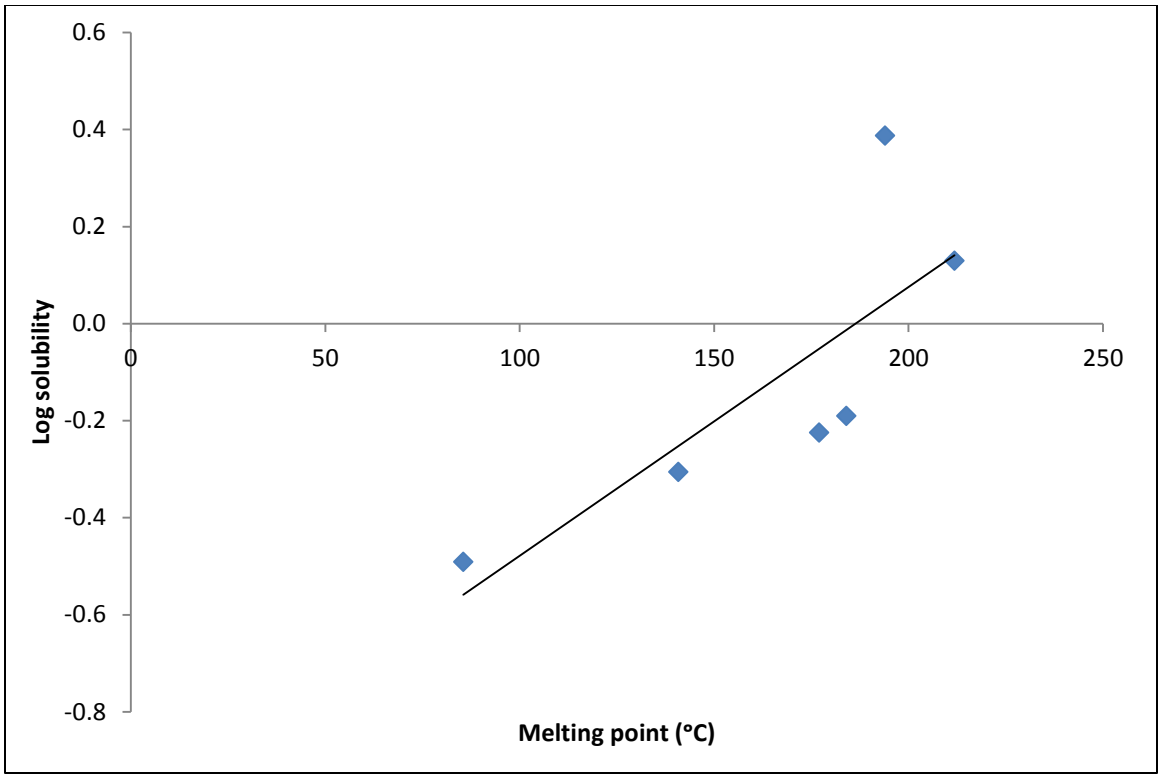

Figure 14. Plot of log solubility versus melting point of salt for halide salts. Equation for line, log y = 0.0055x – 1.0319. $R^2 = 0.6297$.

For the halide salts there appears to be a linear correlation between the melting point and the log solubility, see Figure 14. Interestingly, it has a positive association in comparison to the negative association seen with the benzoate salts – in other words, against all expectations here high melting point correlates to high solubility. For the melting point and the solubility the halide sequence is **I** < **Br** < **Cl**, so polyiodide has a low melting point and an unexpected low solubility. The reason for this reversal from what may be expected from solid-state data may lie in the nature of the solution phase,[17] where chloride is known to have a much greater hydration energy than the heavier halides. Whatever the reason for this anomaly, it highlights the utility of separating the data out into chemically related classes and the risks of assuming that all salt forms of an API follow the same trends.

Investigation of different isostructural groups and effect on solubility

A tree diagram illustrating structural similarity with respect to cation packing in methylephedrine salts was published in reference 18. It has been updated by adding the structures of the salt forms elucidated for this work and then recalculating all relationships.[37] There are three groups at the bottom of the structure tree diagram which are isostructural with respect to their cation packing and which contain more than two salt forms, see figure 15. These groups were examined for any trends or similarities in the data, as it may be expected that isostructural groups should have greater internal similarity with respect to other structures, due to their packing similarities.. Group 4, the enantiopure benzoates **2FBMePD**, **4CBMePD**, **oTolMePD** and **pTolMePD** which have identically clustered structures at the 15 cation level, has a linear correlation between melting point and log solubility, Figure 16, with a R^2 value of 0.8965. The linear equation is log y = -0.0208x + 2.5071 with errors of 0.0050 and 0.7291 on the gradient and intercept respectively. Group 5, which consists of the racemic benzoates **3CBRMePD**, **3FBRMePD**, **3NBRMePD** and **oTolRMePD** shows a similar linear correlation, Figure 17. The group 5 equation is log y = -0.0299x + 3.2922 with R^2 = 0.9591. For both groups 4 and 5 the correlation lines observed are closely related to that seen above for the collective benzoate salts group, however both lines are more accurate than the collective line, with a much better correlation. This indicates that similarity in packing structure leads to greater similarity in property behaviour.

For group 6 the structures that were isostructural for all 15 cations in a cluster were the enantiopure benzoates **2NBMePD** (the sole hydrate in the group), **3ABMePD** and **3FBMePD**. For the analysis we also added to the group the closely related structures of **4HBSMePD**, **4NBMePD** and **4NBRMePD**, see Figure 15. These additions make the group chemically varied, as they include both enantiopure and racemic cations and a sulfonated anion in addition to the benzoates. Excluding the one hydrated structure, a linear correlation between melting point and solubility is found for these chemically diverse species. The linear correlation has the equation log y = -0.0376x + 5.2441 with R^2 = 0.6444, see Figure 18. The lower R value than for structural groups 4 and 5 presumably reflects the greater structural and chemical diversity of group 6. The correlation observed for group 6 also implies that similarity in cation packing leads to similarity in solubility regardless of the counterion, be it a sulfonate or benzoate.

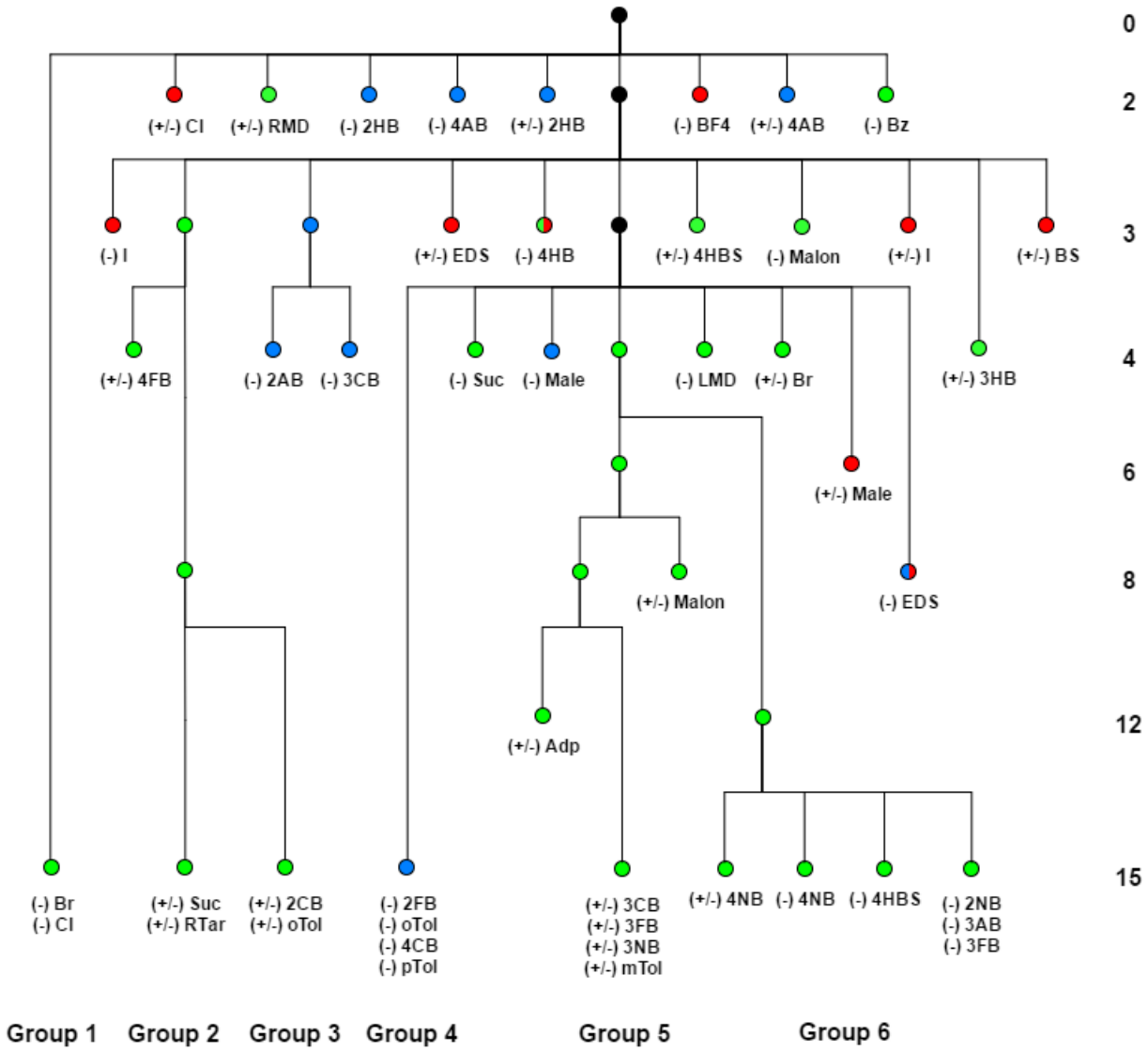

Figure 15. Updated tree diagram showing similarities in packing of cations. Coloured dots indicate different conformations of the molecular cation, as described previously.[18] Green dots = molecular conformation a, red dots = molecular conformation b, blue dots = molecular conformation c.

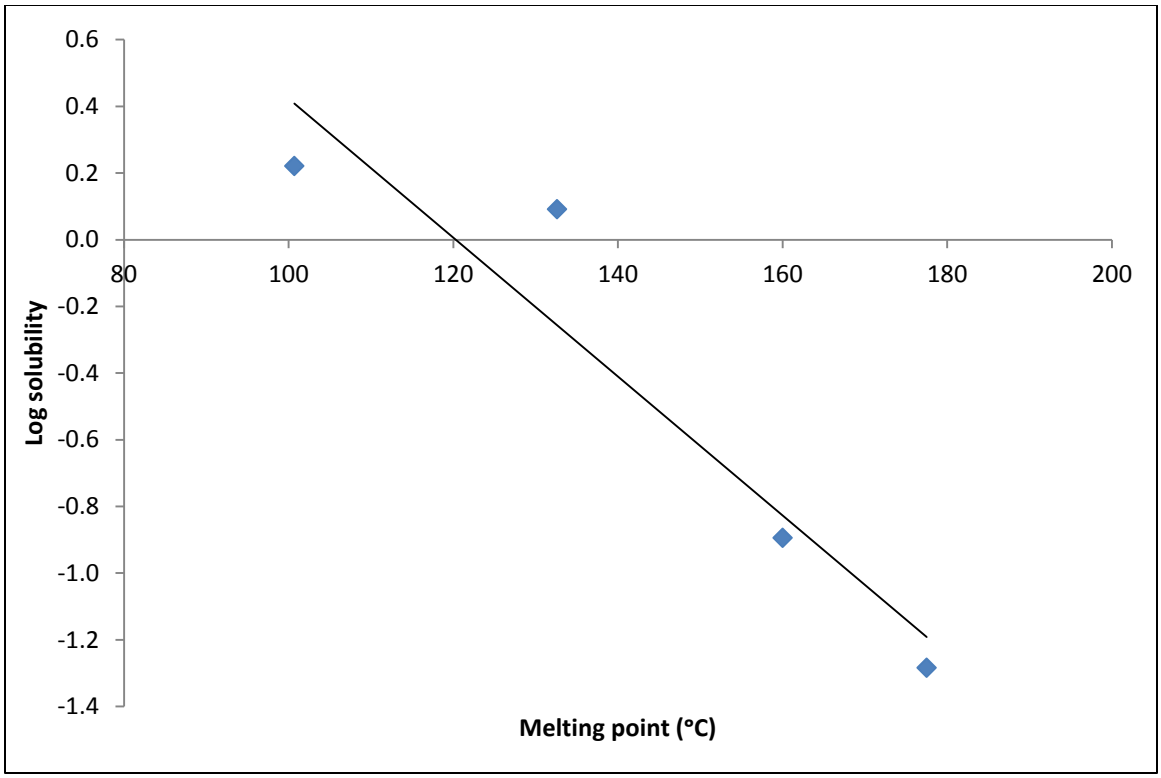

Figure 16. Plot of log solubility versus melting point of salt for methylephedrinium salts of isostructural group 4. log $y = -0.0208x + 2.5071$. $R^2 = 0.8965$.

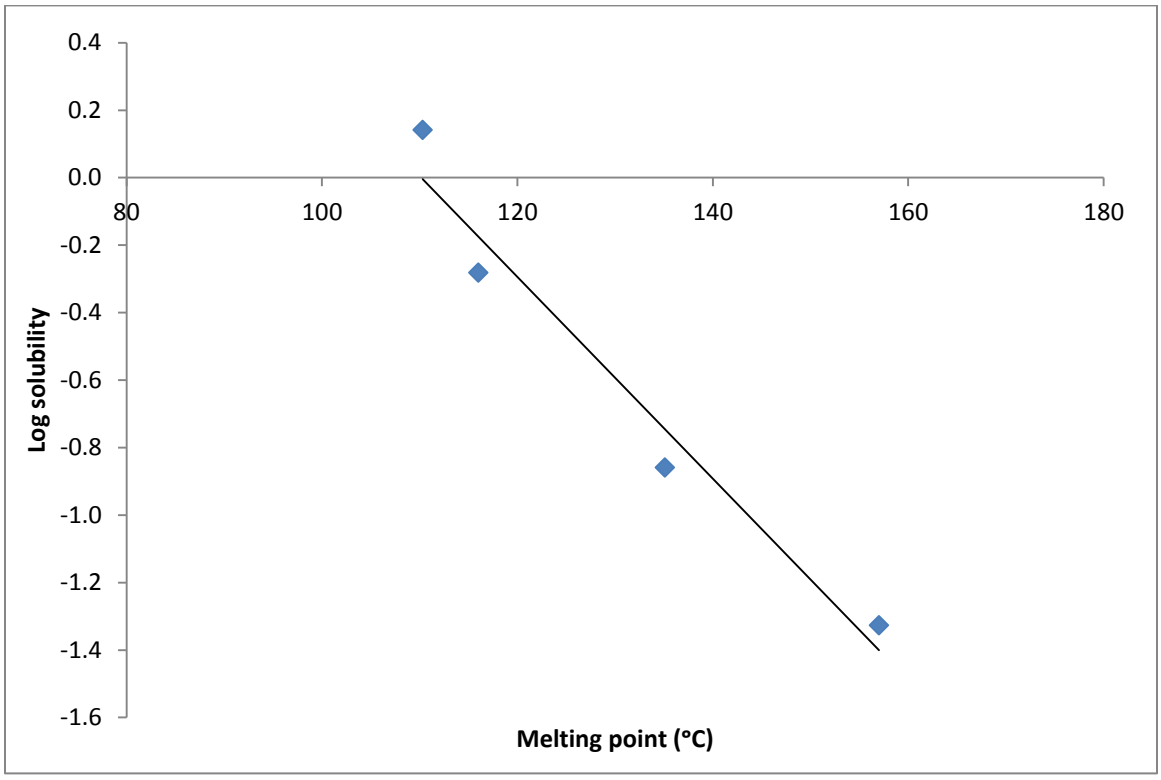

Figure 17. Plot of log solubility versus melting point of salt for methylephedrinium salts of isostructural group 5. log $y = -0.0229x + 3.2922$. $R^2 = 0.9591$.

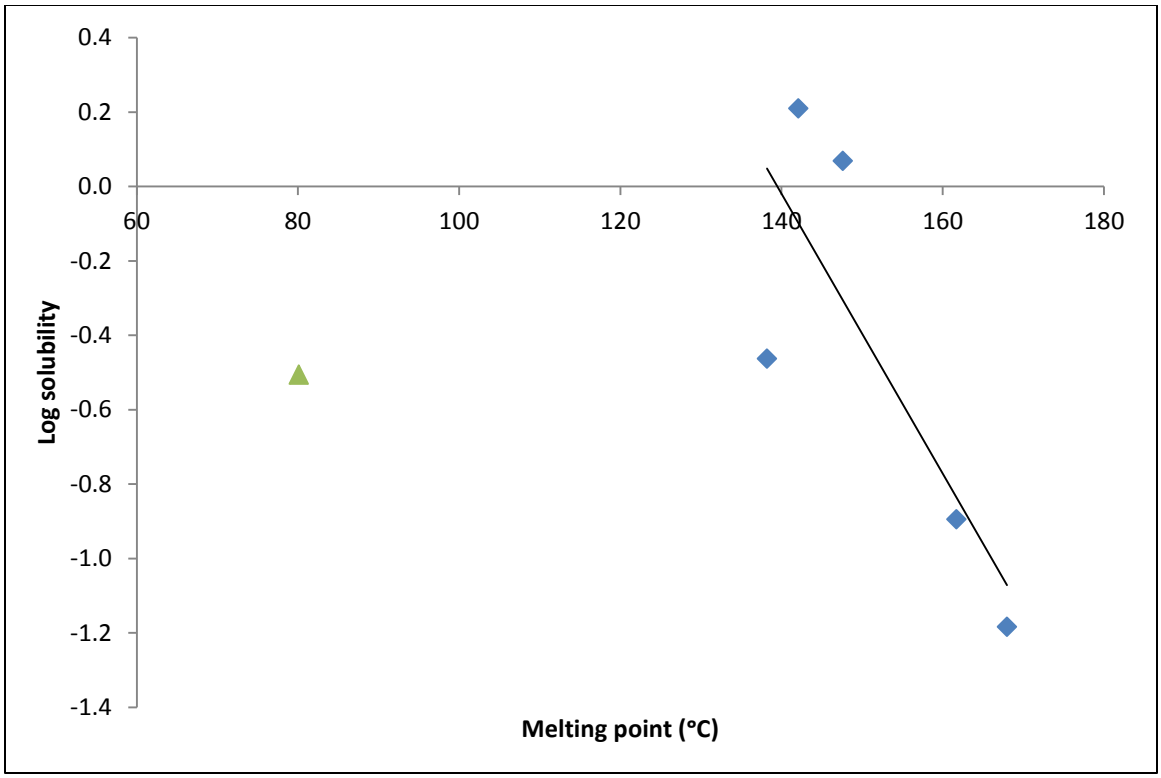

Figure 18. Plot of log solubility versus melting point of salt for methylephedrinium salts of isostructural group 6. The hydrated structure (green triangle) was not included in the line fitting. log y = -0.0376x + 5.2441. R^2 = 0.6444.

Conclusion.

A dataset for use in understanding aqueous solubility in pharmaceutically relevant molecular salts is presented. Crystal structures and solubility values for 51 salt forms, which all share a common cation but with variable anions are presented. Care has been taken to ensure that the solubility values given are phase specific, i.e. they are all tied to a well characterised single crystal structure determination. Other systematic features are that all solubility values were measured under the same conditions and in the same way and that anions were chosen so as to include systematic variation of anion structure. It is hoped that both other groups and our own can use this dataset as a future resource for probing the relationships between anion identity, solid-state structure and solubility of APIs.

In our initial analysis, it was found that identifying correlations between properties was aided by extracting from the data chemically sensible classes e.g. by looking at the salt forms with benzoate-derived anions rather than the set of all anions. This allowed reasonable associations to

be found between solubility and melting point and between melting point of the salt and melting point of the parent acid. Other associations were weaker or non-existent. Interestingly there was no correlation observed between solubility of the salt and solubility of the parent acid. The need to separate compounds into chemically similar groups was illustrated by comparison of the halide and benzoate salt forms. The benzoates gave the expected association of high melting point with low aqueous solubility but the halides unexpectedly reversed the situation. For the halides high melting point correlates with high solubility. This may imply that solid-state structure plays a greater role than solvent interactions for determining solubility of the benzoate salt forms but that the reverse is true for the halide forms. Finally, correlation is further improved by looking only at groups of compounds chosen for similarity in cation packing. The improvement in fit between solubility and melting point data dependant on packing implies an experimentally observed role for packing structure in determining solubility.

Acknowledgements.

The authors thank CNPq (Conselho Nacional de Desenvolvimento Cientifico e Tecnologico) for funding a studentship (LSM, 206093/2014-4). We also thank GSK for advice and encouragement and Mr Wullie Arbuckle for help with measurement of aqueous solubility. Crystallographic data for structure **4FBRMePD** was collected by the National Crystallographic Service at the University of Southampton.

Supplementary Information. This consists of; Powder diffraction data for the solids recovered from slurry experiments; Additional correlation graphs and information; and, details of new single crystal diffraction structures reported in cif format.

References.

[1] Stahl, P. H., Wermuth, C. G., Eds. *Handbook of Pharmaceutical Salts: Properties, Selection and Use*s. Wiley-VCH: Zurich, 2008.

[2] Agharker, S.; Lindenbaum, S.; Higuchi, T. *J. Pharm. Sci.* **1976**, *65*¸747.

[3] Parshad, H.; Frydenvang, K.; Liljefors, T.; Sorensen, H. O.; Larsen, C. *Int. J. Pharm.* **2004**, *269,* 157.

[4] Anderson, B. D.; Flora, K. P.; In *The Practice of Medicinal Chemistry*; Wermuth, C. G. Ed.; Academic Press: London, 1996; pp 739-754.

[5] Forbes, R. T.; York, P.; Davidson, J. R. *Int. J. Pharm.* **1995**, *126,* 199.

[6] Streng, W. H.; His, S. K.; Helms, P. E.; Tan, H. G. H.; *J. Pharm. Sci.* **1984**, *73*,1679.

[7] Braga, D.; Chelazzi, L.; Grepioni, F.; Dichiarante, E.; Chierotti, M. R.; Gobetto, R. *Crystal Growth Des.* **2013**, *13*, 2564.

[8] Rajput, L.; Sanphui, P.; Desiraju, G. R. *Crystal Growth Des.* **2013**, *13*, 3681.

[9] Karanam, M.; Choudhury, A. R. *Crystal Growth Des.* **2013**, *13*, 1626.

[10] Martin, F. A.; Pop, M. M.; Borodi, G.; et al. *Crystal Growth Des.* **2013**, *13*, 4295.

[11] Thakuria, R.; Nangia, A. *Crystal Growth Des.* **2013**, *13*, 3672.

[12] Goud, N. R.; Suresh, K.; Nangia, A. *Crystal Growth Des.* **2013**, *13*, 1590.

[13] Sanphui, P.; Bolla, G.; Nangia, A. *Crystal Growth Des.* **291+2**, *12*, 2023.

[14] Huang, X. F.; Zhang, Z. H.; Zhang, Q. Q.; Wang, L. Z.; He, M. Y.; Chen, Q.; Song, G. Q.; Wei, L.; Wang, F.; Du, M. *CrystEngComm.* **2013**, *15*, 6090.

[15] Arlin, J.-B.; Florence, A. J.; Johnston, A.; Kennedy, A. R.; Miller, G. J.; Patterson, K. *Crystal Growth Des.* **2011**, *11*, 1318.

[16] Collier, E. A.; Davey, R. J.; Black, S. N.; Roberts, R. J. *Acta. Cryst.* **2006**, *B62*, 498.

[17] Black, S. N., Collier, E. A., Davey, R. J. & Roberts, R. J. *J. Pharm. Sci.* **2007**, *96*, 1053.

[18] Kennedy, A. R.; Morrison, C. A.; Briggs, N. E. B.; Arbuckle, W. *Crystal Growth Des.* **2011**, *11*, 1821.

[19] Briggs, N. E. B.; Kennedy, A. R.; Morrison, C. A. *Acta Crystallogr.* **2012**, *B68*, 453.

[20] Harned, W. H. *Capturing and Reporting Electronic Data* **2002**, *824*, 66.

[21] Sheldrick, G. M. *Acta Crystallogr*. **2015**, *C71*, 3.

[22] Altomare, A.; Burla, M. C.; Camalli, M.; Cascarano, G. L.; Giacovazzo, C.; Guagliardi, A.; Moliterni, A. G. G.; Polidori, G.; Spagna, R. *J. Appl. Cryst.* **1999**, *32*, 115.

[23] David, W. I. F.; Shankland, K.; van de Streek, J.; Pidcock, E.; Motherwell, W. D. S; Cole, J. C. *J. Appl. Crystallogr.* **2006**, *39*, 910.

[24] Jacques, J.; Collet, A.; Wilen, S. H. *Enantiomers, Racemates, and Resolutions*; Wiley: New York, 1981.

[25] Grant, D. J. W.; Higuchi, T. (1990). In *Solubility Behaviour of Organic Compounds*. New York: Wiley.

[26] Wallach, O. *Liebigs Ann Chem* **1895**, *286*, 90.

[27] Brock, C. P.; Schweizer, W. B.; Dunitz, J. D. *J. Am. Chem. Soc.* **1991**, *113*, 9811.

[28] Meyerhoffer, W. *Ber. Dtsch. Chem. Ges.* **1904**, *37*, 2, 28604.

[29] Chickos, J. S.; Hesse, D. G. *Struct. Chem.* **1991**, *2*, 33.

[30] Estime, N.; Pena, R.; Teychene, S.; Autret, J. M.; Biscans, B. *J. Cryst. Growth.* **2012**, *342*, 28.

[31] Shefter, E.; Higuchi, T. *J. Pharm. Sci.* **1963**, *52*, 781.

[32] Gould, P. L. *Int. J. Pharm.* **1986**, *33*, 201.

[33] Thomas, E.; Rubino, J. *Int. J. Pharm.* **1996**, *130*, 179.

[34] Parshad, H.; Frydenvang, K.; Liljefors, T.; Larsen, C. S. *Int. J. Pharm* . **2002**, *237*, 193.

[35] Good, D. J.; Rodriguez-Hornedo, N. *Cryst. Growth Des.* **2009**, *9*, 2252.

[36] Yalkowsky, S. H.; He, Y. *Handbook of aqueous solubilitry data*; CRC Press: Florida, 2003.

[37] Macrae, C. F.; Bruno, I. J.; Chisholm, J. A.; Edgington, P. R.; McCabe, P.; Pidcock, E.; Rodriguez Monge, L.; Taylor, R.; van de Streek, J.; Wood, P. A. *J. Appl. Crystallogr.* **2008**, *41*, 466.

FOR TABLE OF CONTENTS USE ONLY

Aqueous Solubility of Organic Salts. Investigating Trends in a Systematic Series of 51 Crystalline Salt Forms of Methylephedrine.

Lygia S. de Moraes, [†] Darren Edwards, [‡‡] Alastair J. Florence,[‡] Andrea Johnston,[‡] Blair F. Johnston,[‡] Catriona A. Morrison,[†] and Alan R. Kennedy[*†]

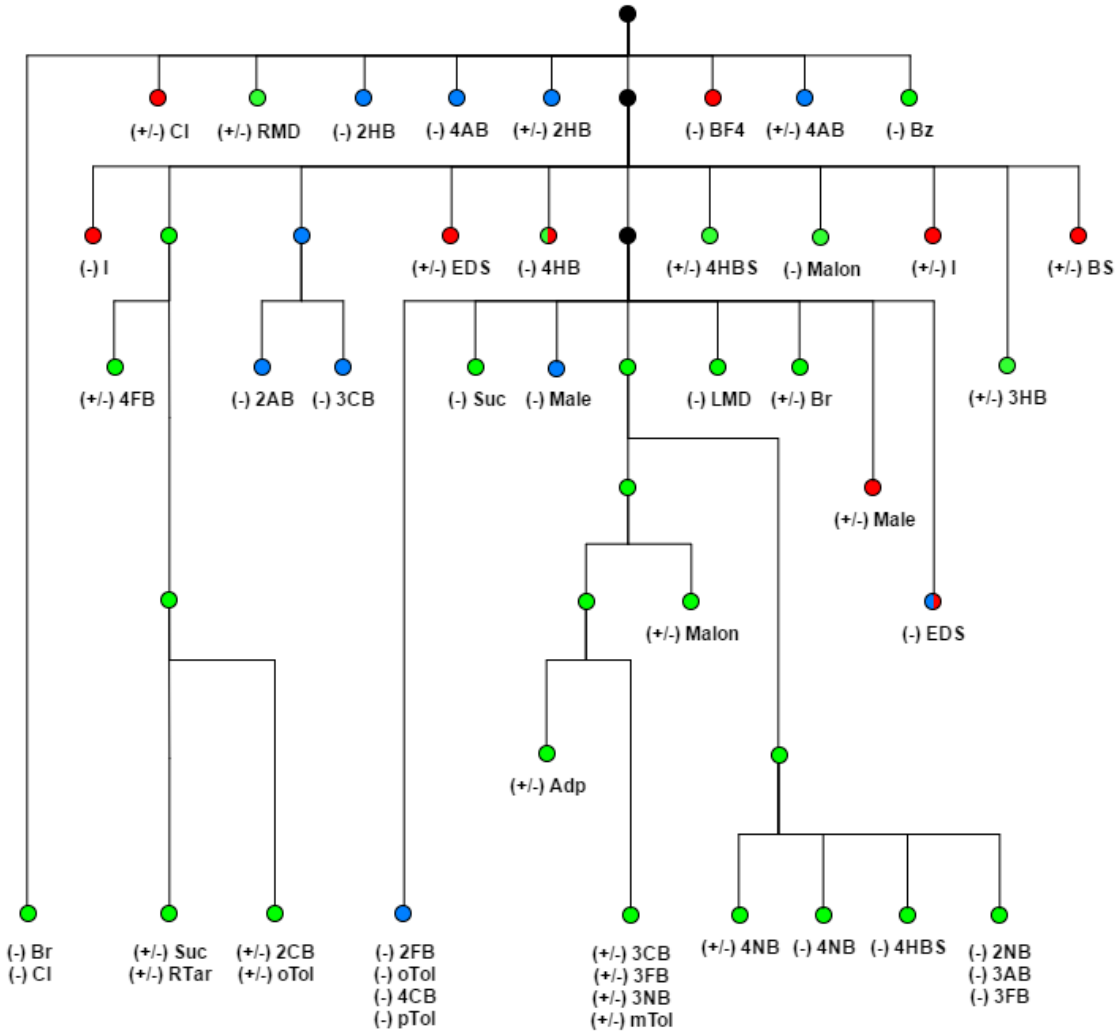

Analysis of aqueous solubility data for 51 salt forms of methylephedrine shows correlation with melting point but not with solubility of the parent free acids. This correlation depends on chemical type, with different associations found for different anion types, for example benzoate anions show negative correlation whilst halides show positive correlation. Correlation is found to be greatest for groups with isostructural cation packing.